Bioprocess Biosyst Eng (2014) 37:1233–1240
DOI 10.1007/s00449-013-1095-z

ORIGINAL PAPER

Physico-chemical characterization and biological response of *Labeo rohita*-derived hydroxyapatite scaffold

S. Mondal · A. Mondal · N. Mandal · B. Mondal · S. S. Mukhopadhyay · A. Dey · S. Singh

Received: 27 August 2013 / Accepted: 10 November 2013 / Published online: 28 November 2013

Abstract The chemically treated *Labeo rohita* scale is used for synthesizing hydroxyapatite (HAp) biomaterials. Thermogravimetric and differential thermal analyses of fish scale materials reveal the different phase changes with temperature and find out the suitable calcination temperatures. The composition and structures of wet ball-milled calcined HAp powders are characterized by Fourier transform infrared spectroscopy, X-ray diffraction, field emission scanning electron microscopy, transmission electron microscopy, energy dispersive X-ray analysis (EDX). The EDX as well as chemical analysis of fish scale-derived apatite materials confirms that the Ca/P ratio is 1.71. The compressive stress, hardness and porosity have been evaluated on sintered HAp biomaterials. The cell attachment on HAp surfaces, cytotoxicity evaluation and MTT assay, which are carried out in RAW macrophage-like cell line media demonstrate good biocompatibility. The histological analysis also supports the bioaffinity of processed HAp biomaterials in Wistar rat model for investigating the contact reaction and stability at the artificial or natural prosthesis interface.

Keywords *Labeo rohita* scale · Hydroxyapatite · Biocompatibility · Cytotoxicity · In vivo

S. Mondal · N. Mandal · B. Mondal (✉)
Centre for Advanced Materials Processing, CSIR-Central Mechanical Engineering Research Institute, Mahatma Gandhi Avenue, Durgapur 713 209, India
e-mail: bnmondal@rediffmail.com; bnmondal@cmeri.res.in

A. Mondal
Department of Biotechnology, Heritage Institute of Technology, Kolkata, India

S. S. Mukhopadhyay · A. Dey
Department of Biotechnology, National Institute of Technology, Durgapur 713 209, India

S. Singh
CSIR-Centre for Cellular and Molecular Biology, Hyderabad, India

Introduction

Fish as a diet has several nutritional and therapeutic benefits for health. The most important constituents of fish as food are protein, fat, carbohydrates, sodium, potassium, calcium, magnesium, vitamin B6 and vitamin B12, which help in maintaining good health as well as the central nervous system of a body [1]. Apart from its nutritional values, fish waste like scale, fin and bone is an important source of hydroxyapatite (HAp) and collagen biomaterials. Each scale consists of two distinct regions: an external (osseous) layer and an internal fibrillary plate. In the upper external layer, collagen fibers are randomly arranged and embedded in a proteoglycan matrix. The collagen fibers are produced within the fibrillary layer by scleroblasts located at the base of the scales. Mineralization of the scales occurs continuously throughout the life of the organism. The external layer is initially mineralized with matrix vesicles and calcium phosphate-based materials are deposited biologically on the layer matrix. HAp is the most stable calcium phosphate salt at normal temperatures with a pH between 4 and 12 [2]. It is an important material of great interest in protein chromatography applications, waste water treatment processes and suitable scaffold materials [3, 4]. HAp is also considered as a model compound to study biomineralization phenomena [5, 6]. There is an intensive attempt for the development of well-defined HAp crystals toward physicochemical behavior in vitro and

in vivo studies for reconstructive bone replacement and other medical applications [7, 8]. In literature, several methods of preparation of HAp crystals from bio-wastes have been reported, including solid-state reactions, crystal growth under hydrothermal reaction, layer hydrolysis of other calcium phosphate salts, sol–gel crystallization [9–15]. Due to low production cost and worldwide availability, the researchers [16] are concentrated on the use of fish scale bio-waste for the processing of HAp crystal [17]. Many processing technologies have been employed to obtain porous ceramics for bone tissue engineering from different bio-wastes. In tissue repair application, the macropores and highly interconnected networks are required for the growth of surrounding host tissues. The porosity of filler scaffold is about 30–33 % which is also similar to the results reported by Gross et al. [18]. The optimal scaffold design and fabrication techniques must be able to create porous structures adequate for attaining the desired mechanical function and mass transport properties [18, 19]. In this paper, an attempt has been made to synthesize HAp powder from *Labeo rohita* scale. The powder is characterized through thermogravimetric analysis, X-ray diffraction (XRD) and Fourier transform infrared spectroscopy (FTIR), etc. The mechanical properties of the sintered HAp have been evaluated for development of porous scaffold. The cell attachment on HAp surfaces, cytotoxicity evaluation and MTT assay on RAW macrophage cell line media are carried out to demonstrate good biocompatibility.

Methods and materials

Synthesis and characterization of hydroxyapatite powder from fish scale

Labeo rohita scales are used as raw material for HAp processing. Scales are initially washed thoroughly with water to discard impurities and then deproteinized by solvent system. The cleaned de-protienated scale is calcined at 700–800 °C to synthesis HAp ceramics after differential thermal analysis of scale from room temperature to 1,200 °C by NETZSCH Jupiter STA 491 at a heating rate of 10 °C/min. XRD Analysis of HAp powder is performed at the scanning range of $2\theta = 20°–80°$ with CuK_{α} target by Shimadzu, XRD-6000 instrument. The crystallographic phases of HAp with different temperatures are recorded and confirmed the HAp using standard JCPDS files. FTIR analysis is carried out at the scanning range of 4,000–400 cm^{-1} (Shimadzu IR Prestige—21, Japan) to determine functional groups present in HAp powder. FESEM and EDX (Model No: SUPRA 40, CARLZEISSSMT, Oxford) analyses reveal the compositional and morphological structure of green as well as sintered powder of HAp. Quantitative energy dispersive X-ray is also performed to confirm the Ca/P ratio of the sample apart from chemical method. Ultrasonic instruments are employed for dispersing and homogeneously distribute the particles into liquids to prepare samples for TEM analysis (TEM, Jeol Gem Microscope). "Image J" software is used to evaluate the typical images of HAp particles.

Preparation of fillers and scaffold

The calcined powder is wet ball-milled for 48 h in planetary mill. The particle size of dried milled powder is measured in Malvern particle size analyzer. The average size of the particle is ~0.5 μm. Triton–X surfactant is added drop wise to the dried ball-milled powders to make a paste for injection molding. The sample is prepared as small rod-shaped fillers with 2 mm diameter and 4 mm long. The fillers are then dried at 80 °C for several hours. Finally, the dried samples are sintered at 1,200 °C for 2 h. Alternatively, hydroxyapatite samples are mixed well with requisite amount of starch porogen and compacted with unidirectional pressure at 200–250 MPa to make 12 mm dia. The sample was sintered at 1,200 °C for crystallographic phase determination as well as physico-mechanical property evaluation. The process flow of fish scale-derived HAp scaffold development and in vivo bio-implantation is shown in Fig. 1.

Results and discussion

Differential thermogravimetric analysis

The DTA/TG analysis reveals the phase transformation and determines the weight loss with respect to temperatures. Two major and one minor mass losses are distinctly observed as depicted in Fig. 2. The first major weight loss is observed in the range of 100–400 °C, on the heating process from room temperature to 1,200 °C. This mass loss is reported as near about 4.56 % of the sample taken for experimentation. The first mass loss process may be due to the removal of adsorbed water from the surface and interparticle spaces [17]. Other exothermic peaks at ~407 and 709 °C correspond to weight losses about 0.86 and 0.17 %, respectively. The weight loss at the range of 400–500 °C is due to the combustion of organic materials. However, there is a minor weight loss observed on heating up beyond 710° to 1,200 °C, which indicates better thermal stability of the sample in this range.

X-ray diffraction analysis

The crystalline phase analysis of the HAp powder from fish scale is carried out by XRD studies. The XRD of HAp

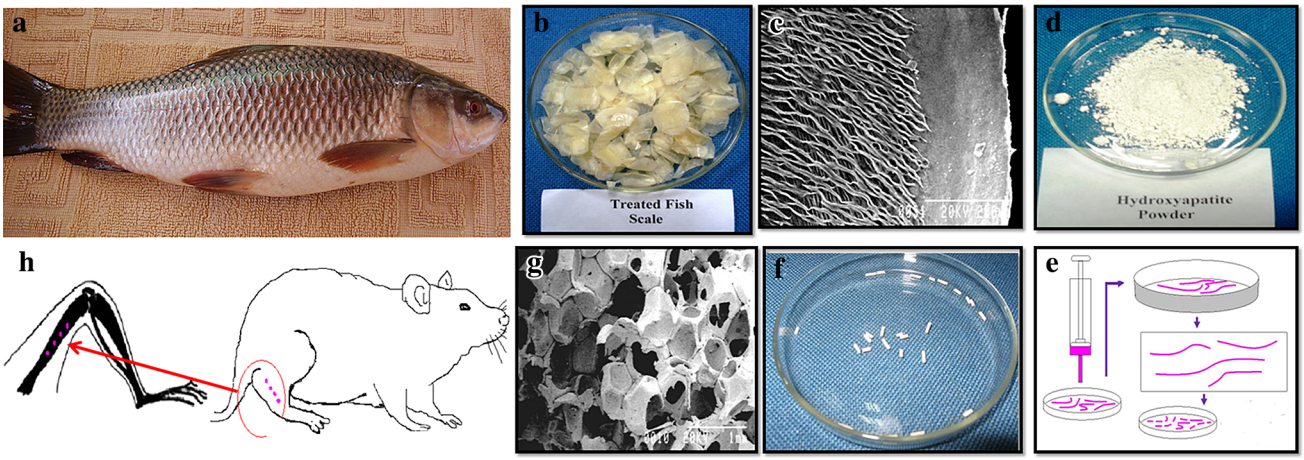

Fig. 1 Pictorial representation of **a** fish *Labeo rohita*, **b** chemically treated dried fish scale, **c** scanning electron microscopy of treated fish scale, **d** synthesized HAp powder, **e** fabrication of small fillers by injection press molding, **f** sintered fillers, **g** SEM images of porous fillers, **h** schematic representation of fillers in rat model

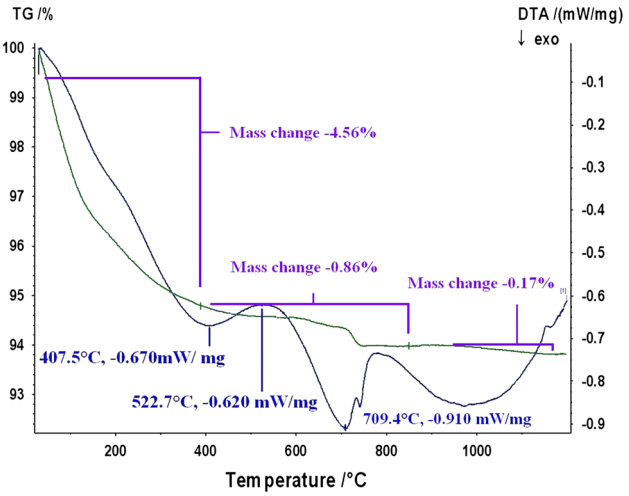

Fig. 2 TG/DT analysis of HAp powder

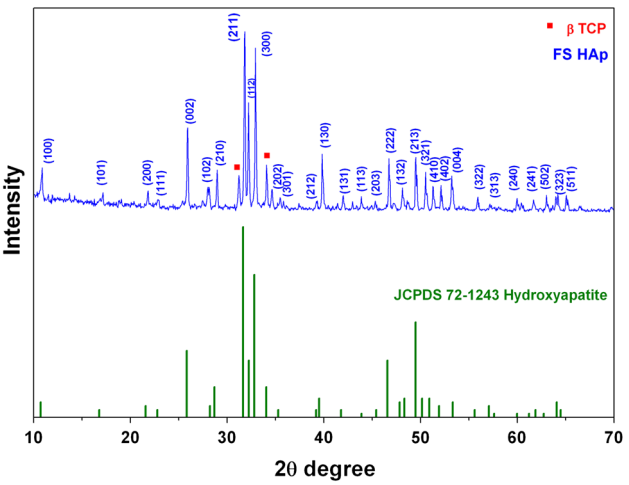

Fig. 3 XRD analysis of HAp powder

indicates the visible crystalline nature of typical apatite crystal structures. It is also noticed that crystallographic behavior of HAp resembles to that of XRD pattern of biological apatite [20] which is shown in Fig. 3. However, the pattern of the fish scale-derived HAp powder peaks corresponds to the JCPDS card No. 72-1243 of pure HAp. The highest intensity peak of synthesized powder is in the plane of 211 and it resembles to the pure HAp crystal XRD characteristics. The two minor β-TCP peaks are observed at 31° and 34° after sintering at 1,200 °C.

Fourier transform infrared spectroscopy analysis

FTIR spectroscopy is employed to characterize the different functional groups of HAp [Ca_{10} $(PO_4)_6(OH)_2$]. FTIR spectrum of HAp powder calcined at 700 °C is recorded in the range of 4,000–400 cm^{-1} as shown in Fig. 4. The characteristics of FTIR peaks in the wave range 570–632 cm^{-1} resemble asymmetric bending vibration of P–O band of HAp materials, whereas the peak at 960–965 cm^{-1} is due to symmetric stretching vibration of P–O band of PO_4^{3-} ion. The spectral data at the wave number values of 876, 1,412 and 1,451 cm^{-1} suggest the presence of carbonate ion [21] in the prepared HAp materials calcined at 700 °C. The strong peaks at 1,053 and 1,095 cm^{-1} are ascribed to asymmetric stretching mode of vibration of P–O bands of PO_4 tetrahedra [22, 23]. The characteristic frequencies derived from PO_4^{3-} modes are better resolved with increasing temperature. The existence of O–H and C–O bands disappears beyond calcinations temperature of the powder (1,200 °C). But the structural O–H peaks at 1,655 and 3,370 cm^{-1} are predominant with increasing temperature, whereas the existence of C–O bands is reduced significantly. Therefore, sintered HAp

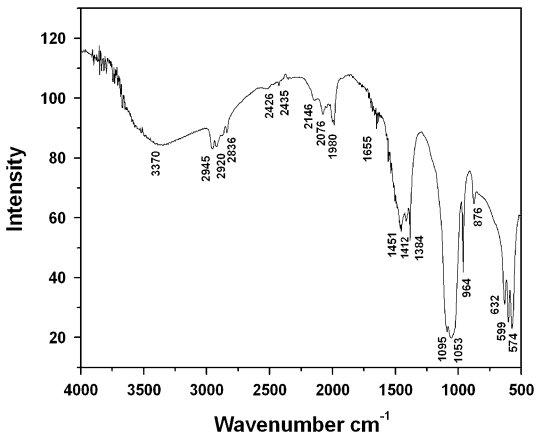

Fig. 4 FTIR analysis of HAp powder

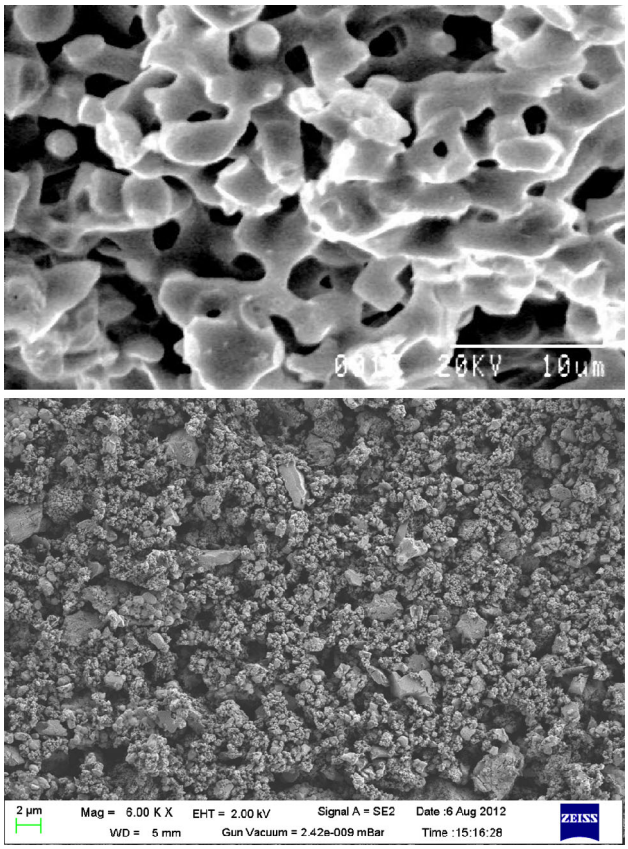

Fig. 5 SEM images of porous HAp scaffold and HAp particles synthesized from fish scale

ceramics synthesized from fish scale beyond 1,200 °C is established.

FE-SEM and EDX analyses

The FE-SEM micrograph of fish scale-derived HAp dried powder and fillers scaffolds is depicted in Fig. 5. The morphology of calcined wet ball-milled dried HAp powder

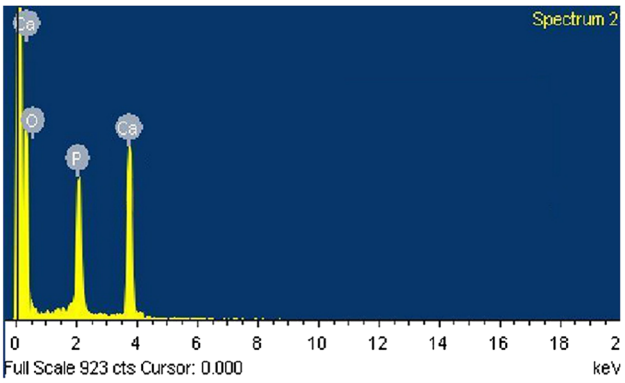

Element	Weight %	Atomic %
O K	53.35	73.36
P K	17.21	12.17
Ca K	29.44	14.47
Total	100	

Fig. 6 EDX analysis of HAp particles

shows soft agglomerated ultrafine particles. The biocompatible powder consists of a uniform porous structure upon compacting at 200–250 MPa with porogen (starch granules Merck). The compacted HAp-sintering surface shows distinct grain boundary with uniform porous structure. EDX analysis of the synthesized HAp powder shows that the ratio of Ca/P is 1.71 as depicted in Fig. 6.

Chemical analysis of Ca/P ratio in fish scale HAp

To perform the chemical analysis, a weighed quantity of hydroxyapatite powder is dissolved in dilute (1:1) nitric acid (HNO_3). Calcium content is determined from an aliquot part of the solution by reverse complexometric titration, i.e., by titration of the excess of complexone III (disodium salt of ethylenediamine tetra-acetic acid) with the use of a solution of nickel(II) chloride in ammonia. Murexide (ammonium purpurate) is used as the indicator for titration.

Phosphorus was determined colorimetrically as the phosphovanadomolybdate complex with a UV–VIS Shimadzu Model spectrophotometer using a wavelength of 420 nm. Phosphorus content is determined by the photometric method on the basis of the formation of yellow phosphomolybdic acid and its subsequent reduction to a blue complex compound in a hydrochloric acid solution of thiocarbamide in the presence of copper (II) sulfate. The error of the analysis is 0.5 % Ca and 0.1 % P [24]. The experiment is repeated thrice to ascertain the Ca/P ratio. The ratio of Ca/P is in the range of 1.70–1.73, whereas the EDX experiment shows 1.71 as depicted in Fig. 6.

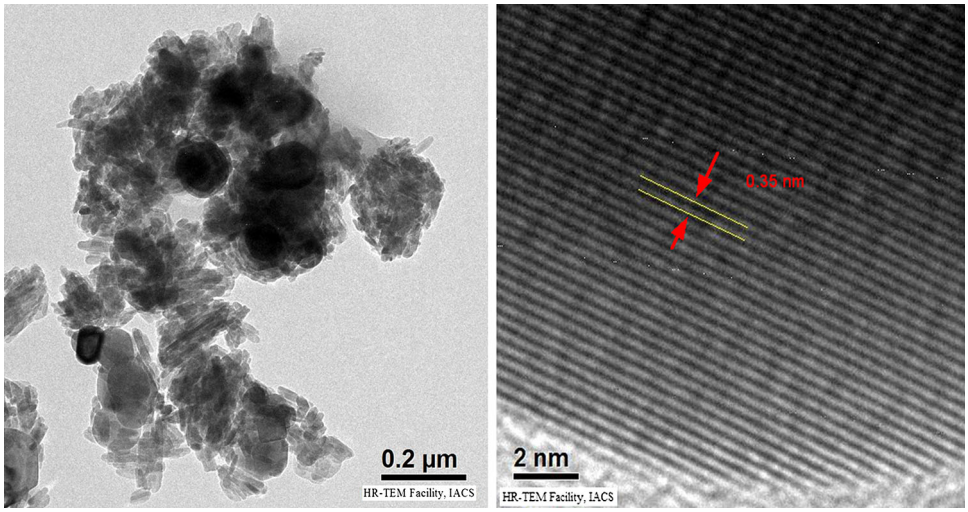

Fig. 7 TEM images of HAp particles and atomic distribution in fringe pattern

Table 1 Mechanical properties of different bone tissues and related materials with references

Tissues	Compressive strength (GPa)	Hardness (GPa)	References
Human tooth (enamel)	~0.25–0.55	~3.3	Orlovskii et al. [26]
Human bone (cortical)	~0.088–0.230	–	Sarsilmaz et al. [27]
Hydroxyapatite	~0.3–0.9	~5.88	Sarsilmaz et al. [27]
Zirconia	~1.7–2	~10.78–11.76	Sarsilmaz et al. [27]
Fish scale HAp	~0.8	~1.08	Experimental

TEM analysis

Actual particle shape analysis is a complex process in powder technology and till now there is no shape factor available which will clearly differentiate all possible kinds of shape [25]. In spite of these complexity till date, TEM and SEM both instrumentation are highly efficient to determine particle shape and size. In this study, HAp particle size, shape and morphology are observed by TEM images. According to TEM images, small rice-shaped particles are observed in plenty and some spherical large particles are also observed. The fringe pattern of HAp interatomic space is about 0.35 nm as shown in Fig. 7.

Mechanical characterization

The compacted samples are optically polished to measure the micro hardness with 100 g load. The average Vickers hardness (HV) of HAp sample is observed about 115 HV. The average porosity is observed about 30–35 %. Compressive stress of the hydroxyapatite samples is tested by UTM (Make: Tinius Olsen, U.K). Sample's L/D ratios are between 4 and 6. Loads are applied with extension and compression rate of 0.2 mm/s. The ultimate compressive stress of the developed HAp scaffold has reached up to ~0.8 GPa which is better than cortical human bone [26]. Different human skeletal parts and their comparative features of mechanical characterization are shown in Table 1.

Biocompatibility study

In vitro cytotoxicity study of the developed HAp is carried out by culturing RAW macrophage-like cells in a contact mode. RAW cells are cultured in RPMI media and seeded on the six well culture plates at their exponential phase of growth at a density of 10^5 cells/200 μl. The cells are allowed to attach to the films surface for 6 h in 5 % CO_2 incubator at 37 °C. HAp powder samples as well as fillers/plates are utilized for in vitro testing. The samples of different weights (100, 200, 400 μg) are placed into RPMI culture media. RPMI supplemented with 10 % fetal calf serum (FCS) is added to each well to keep the cell-containing samples submerged. The culture plates are incubated for 24 h at 37 °C in a humidified atmosphere of 5 % CO_2 in air. Two set of experiments are performed for this cell viability assay. One set of experimental plates is further incubated for more than 48 h in the same atmospheric condition with equal-interval fresh media incorporation in the culture plates. After 72 h incubation in cell culture media samples are stained with trypan blue and observed under inverted microscope as depicted in Fig. 8. In Fig. 8a red trigonal symbol shows living healthy RAW cell lines attached on culture vessels where as yellow arrow indicates the hydroxyapatite particles synthesized from fish scales. Software analysis of images 8(b) distinctly defines the attached cells (blue arrow) and the hydroxyapatite particles (indigo trigonal) as shown in Fig. 8b. Attached living healthy cells prominently show

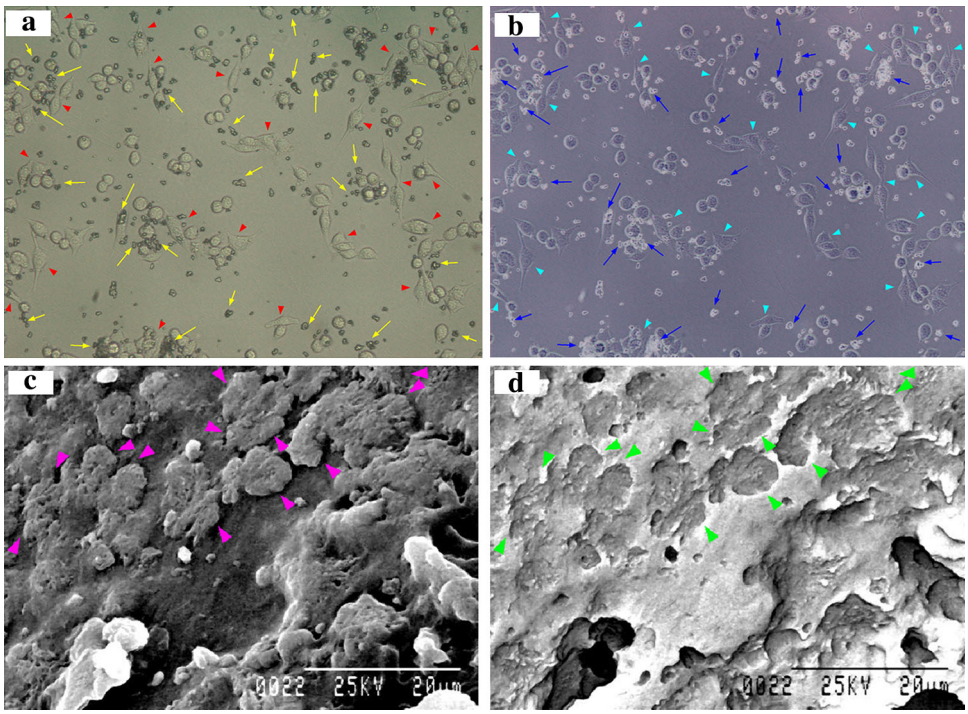

Fig. 8 Cytotoxicity evaluation in RAW cell line media and attachment of cells on HAp surface

Table 2 Results of MTT assay: percentage of cell viable

HAp concentration (µgm/ml)	Viable cell (%)
100	131
200	125
400	128

their protoplasm in Fig. 8b. The experimental result reveals the non-immunogenic effect of hydroxyapatite particles toward cell lines (Table 2).

On the other hand, second set of experimental plate is utilized for MTT assay. After 24 h incubation, MTT (10 µl) is added to each well at a strength of 10 % (v/v) and incubated for further 4 h at 37 °C. Subsequently, the media containing MTT is removed, and 100 µl of DMSO (dimethylsulfoxide) is added to dissolve the formazan crystals. The plates are agitated for 5 min and read at 550 nm on a scanning multi-well spectrophotometer plate reader (Biorad, USA). *t* test is performed for statistical significance analysis and a *P* value of <0.05 is determined to represent a significant difference. The percentage of cell viable is expressed as

$$\frac{\text{Absorbance of treated cells}}{\text{Absorbance of controlled cells}} \times 100\ \%.$$

Cell attachment study

HAp blocks are used for in vitro cell attachment studies. HAp blocks are sterilized and then RAW cell lines are used in RPMI cell culture media for this study. After 72 h incubation samples cell culture media is decanted and washed thoroughly with phosphate buffer solution (PBS). After washing 2 % paraformaldehyde solution is utilized for cellular fixation. Figure 8c shows SEM image attached cells on to the HAp surface. This study reveals that cells can be attached on the HAp surface which would be utilized as scaffold material for tissue engineering application. Software analysis of Fig. 8c shows the exact attached location of cell lines on hydroxyapatite surface as shown in Fig. 8d. This experimental result shows the bioaffinity of synthesized hydroxyapatite particles toward cell line.

Histological analysis

In the present pilot study, histological analysis [27, 28] is performed in Wistar rats. Wistar rats are easy to handle and their femur is brittle but not fragile during drilling. Skeletally mature 3-months-old female Wistar rats of body weight 150–200 g from the animal house are used for the experiment. The animals are maintained at standard environmental conditions (temperature 22–25 °C, humidity 40–70 % with 12:12 dark/light photoperiod) approved by the Committee for the Purpose of Control and Supervision of Experiment on Animals (CPCSEA) whereas all the experimental protocols are approved by IAEC, CCMB.

Animals were anesthetized with ketamine and xylazine with a dose of 40 mg and 5 mg/kg body weight, respectively. Lateral and median aspect of the femur is cleaned. An incision is made to cut open the skin on the dorsal aspect above the femur. A careful incision is then made to

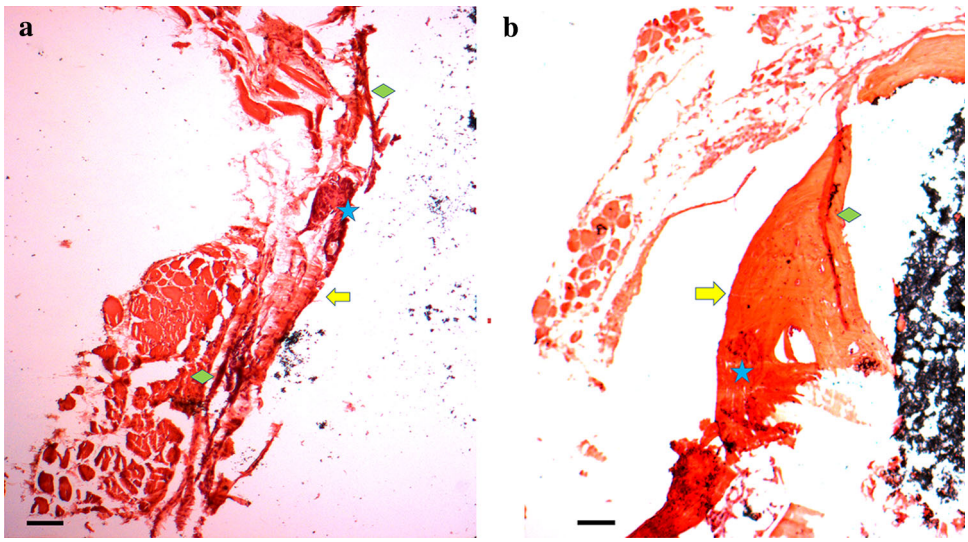

Fig. 9 Histological analysis of femur bone of Wistar rat with HAp prosthetic fillers. **a** and **b** shows Bone formation on hydroxyapatite implant (*arrow*) shows lining cells. Healing is on progress in 3 months sample. Some integration of cells are seen, cell infiltration on materials are also observed (*star*). Pre-osteoblast cells appear which could be identified by mono nuclear cells wih prominent nulceoli and deeply stained cytoplasm (*rhombus*). Each bar (*thick line*) represents 50 μm

cut open the biceps femoris muscles to expose femur bone. A Pediatric bone driller is used to make a hole of 5 mm in the dorsal surface of femur without touching the bone marrow thus preventing any hemorrhage. The drilled femur of control animal is left unfilled, whereas in experimental group the HAp rods are fixed to fill up the gaps. The muscle layer is stitched with simple interrupted suture using absorbable materials and skin is closed using non-absorbable suture materials. Povidone, iodine ointment is applied externally for 3 days. At the end of the experiment after 3 months, the animals are sacrificed by overdose of CO_2. Detail necropsy is done and femur bone is collected and fixed in 10 % formalin [29]. Fixed bone is decalcified with EDTA before embedding in paraffin wax. Fixed and paraffin embedded bones are cut at 5 μm thickness, stained with Hematoxylin and Eosin following standard procedure and examined under light microscope as shown in Fig. 9a.

The response of tissues and the implanted material is assessed. Trauma regions are being recovered by healing new cells as cell infiltration on materials is observed. Deeply stained region may conclude the presence of pre-osteoblast cells because this type of cells consists of mono nucleus with prominent nucleoli. In some regions, new cell linings are appeared which may be the result of osteo-conduction as shown in blue arrow in Fig. 9b.

Conclusion

- *Labeo rohita* scale-derived HAp is almost similar to the structure of pure HAp.
- The porous HAp scaffold with ~30 % porosity shows considerable improvement in compressive strength ~0.8 GPa which may be suitable for nutrient and biological fluid transportation for in vivo system.
- Cytotoxicity analysis of HAp particles and MTT assay indicates no cytotoxic effects on macrophage-like RAW cell line media.
- The histological analysis concludes cell infiltration and integration in HAp fillers which is a good result of bioactivity.
- Cellular attachment on HAp surface reveals that hydroxyapatite microsphere is able to support cell lines to adhere and proliferate.

Acknowledgments The authors would like to express their gratitude to Director, CSIR-CMERI for his kind permission to publish this paper. The authors are thankful to Dr. Syamal Roy, Head of the department of Immunology and infectious diseases at IICB Kolkata for their kind support for cell culture, toxicity studies. The authors are also indebted to CSIR-Centre for Cellular and Molecular Biology (CSIR-CCMB), Hyderabad for histological and in vivo studies. The financial support from CSIR is highly acknowledged.

References

1. Kawarazuka N (2010) The contribution of fish intake, aquaculture, and small-scale fisheries to improving nutrition: a literature review. The World Fish Center Working Paper No. 2106. The World Fish Center, Malaysia
2. Koutsopoulos S (2002) Synthesis and characterization of hydroxyapatite crystals: a review study on the analytical methods. J Biomed Mater Res 62:600–612
3. Zhang J, Zhang W, Bao T, Chen Z (2013) Mussel-inspired polydopamine-assisted hydroxyapatite as the stationary phase for capillary electrochromatography. Analyst. doi:10.1039/c3an01668d
4. Intapong S, Raksudjarit A (2013) Treatment of agricultural wastewater using porous ceramics composite of hydroxyapatite and silica. Adv Mater Res 622–623:915–918
5. Kim MH, Himeno T, Kawashita M, Kokubo T, Nakamura T (2004) The mechanism of biomineralization of bone-like apatite on synthetic hydroxyapatite: an in vitro assessment. J R Soc Interface 1:17–22

6. Zhang HM, Wu B (2011) Biomineralization of the hydroxyapatite with 3D-structure for enamel reconstruction. Adv Mater Res 391–392:633–637
7. Koutsopoulos S, Demakopoulos J, Argiriou X, Dalas E, Klouras N, Spanos N (1995) Inhibition of hydroxyapatite formation by zirconocenes. Langmuir 11:1831–1834
8. Ozawa M, Suzuki S (2002) Microstructural development of natural hydroxyapatite originated from fish-bone waste through heat treatment. J Am Ceram Soc 85:1315–1317
9. Dorozhkin Sergey V (2010) Bioceramics of calcium orthophosphates. Biomaterials 31(2010):1465–1485
10. Venkatesan J, Ji Qian Z, Ryu B, Vinay Thomas N, Kim SK (2011) A comparative study of thermal calcination and an alkaline hydrolysis method in the isolation of hydroxyapatite from *Thunnus obesus* bone. Biomed Mater 6(3):035003
11. Bardhan R, Mahata S, Mondal B (2011) Processing of natural resourced hydroxyapatite from egg shell waste by wet precipitation method. Adv Appl Ceram Struct Funct Bioceram 110:80–86
12. Liao CJ, Lin FH, Chen KS, Sun JS (1999) Thermal decomposition and reconstitution of hydroxyapatite in air atmosphere. Biomaterials 20:1807–1813
13. Yamasaki N, Kai T, Nishioka M, Yanagisawa K, Ioku K (1990) Porous hydroxyapatite ceramics prepared by hydrothermal hot pressing. J Mater Sci 9:1150–1151
14. Cheng PT (1987) Formation of octacalcium phosphate and subsequent transformation to hydroxyapatite at low supersaturation: a model for cartilage calcification. Calcif Tissue Int 40:339–343
15. Piccirillo C, Silva MF, Pullar RC, Braga da Cruz I, Jorge R, Pintado MME, Castro PML (2013) Extraction and characterisation of apatite- and tricalcium phosphate-based materials from cod fish bones. Mater Sci Eng C 33(1):103–110
16. Boutinguiza M, Pou J, Comesaña R, Lusquiños F, de Carlos A, León B (2012) Biological hydroxyapatite obtained from fish bones. Mater Sci Eng C 32(3):478–486
17. Mondal S, Mahata S, Kundu S, Mondal B (2010) Processing of natural resourced hydroxyapatite ceramics from fish scale. Adv Appl Ceram Struct Funct Bioceram 109:234–239
18. Gross KA, Rodríguez-Lorenzo LM (2004) Biodegradable composite scaffolds with an interconnected spherical network for bone tissue engineering. Biomaterials 25(20):4955–4962
19. Miranda P, Saiz E, Gryn K, Tomsia AP (2006) Sintering and robocasting of β-tricalcium phosphate scaffolds for orthopaedic applications. Acta Biomater 2(4):457–466
20. Bose S, Roy M, Bandyopadhyay A (2012) Recent advances in bone tissue engineering scaffolds. Trends Biotechnol 30(10): 546–554
21. Liu Q, Huang S, Matinlinna JP, Chen Z, Pan H (2013) Insight into biological apatite: physiochemical properties and preparation approaches. Biomed Res Int. doi:10.1155/2013/929748 (Article ID 929748)
22. Panda RN, Hsieh MF, Chung RJ, Chin TS (2003) FTIR, XRD, SEM and solid state NMR investigation of carbonated hydroxyapatite nano particles synthesized by hydroxide gel technique. J Phys Chem solids 64:193–199
23. Fathi MH, Hanifi A, Mortazavi V (2008) Preparation and bioactivity evaluation of bone-like hydroxyapatite nanopowder. J Mater Process Technol 202(1–3):536–542
24. Garbuz VV, Dubok VA, Kravchenko LF, Kurochkin VD, Ul'yanchich NV, Kornilova VI (1998) Analysis of the chemical composition of a bioceramic based on hydroxyapatite and tri calcium phosphate. Powder Metall Metal Ceram 37(3–4):193–195
25. Pourghahrsamani P, Forssberg E (2005) Review of applied particle shape descriptors and produced particle shapes in grinding environments: part II: particle shape. Miner Process Extr Metall Rev 26:145–166
26. Orlovskii VP, Komlev VS, Barinov SM (2002) Hydroxyapatite and hydroxyapatite-based ceramics. Inorg Mater 38(10): 973–984
27. Sarsilmazb F, Orhanb N, Unsaldia E, Durmusa AS, Colakogluc N (2007) A polyethylene- high proportion hydroxyapatite implant and its investigation in vivo. Acta Bioeng Biomech 9(2):9–16
28. Flautre B, Anselme K, Delecourt C, Lu J, Hardouin P, Descamps M (1999) Histological aspects in bone regeneration of an association with porous hydroxyapatite and bone marrow cells. J Mater Sci Mater Med 10:811–814
29. Sujatha R, Isnik S, Guha A, Mahesh Kumar J, Sinha A, Singh S (2012) Evaluation of nano-biphasic calcium phosphate ceramics for bone tissue engineering applications: in vitro and preliminary in vivo studies. J Biomater Appl 27:565–575